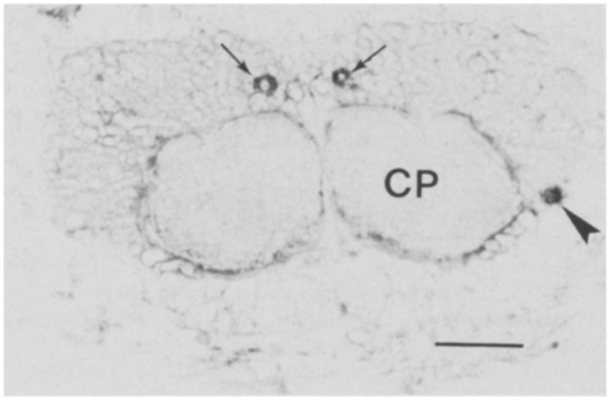

Horizontal section of the brain of the 5th larval instar of the hoverfly. 2 PP immunoreactive cells (arrows), 1 in each protocerebrum hemisphere, located in the mid-anterior position to the corpora pedunculata (CP). At the bottom to the right (arrow head) another PP immunoreactive cell is seen in latero-posterior situation to the corpora pedunculata. The outer nerve fiber layers of the corpora pedunculata show nonspecific staining. Scale bar = 21 µm.

immunoreactive nerve fibers could be detected. However, the outer nerve fiber layers of the corpora pedunculata showed a weak staining. The specificity of the immunostaining of these cells was confirmed by the following observations: a) no positive staining was seen when the first-layer antiserum was replaced by normal rabbit serum; b) the pre-incubation of anti-BPP with rabbit anti-Clq complement had no effect on the positive result obtained; and c) the immunostaining was abolished completely after preincubation of the antiserum with 125 µg of BPP (a gift from Dr R.E. Chance) per ml of the diluted antiserum. On the other hand, the weak staining of the outer nerve fibers of the corpora pedunculata appeared to be nonspecific, being observed after the previously mentioned negative controls.

The present observations confirm previous reports[2,3] on the occurrence of PP cells in the brain of insects. Furthermore, the absence of PP immunoreactive nerve fibers to convey the secretory products of the PP cells to the distant neurohaemol organ or other organs is in agreement with the assumption[3] that these cells may have a local function, acting on the neighbouring nerve tissues.

1 Support by a grant from the Swedish Medical Research Council (project No. 12X-102) and by a Swedish Institute scholarship.
2 R. Yui, T. Fujita and S. Ito, Biomed. Res. *1*, 42 (1980).
3 H. Duve and A. Thorpe, Cell Tissue Res. *210*, 101 (1980).
4 M. El-Salhy, R. Abou-El-Ela, S. Falkmer, L. Grimelius and E. Wilander, Regul. Peptides *1*, 187 (1980).
5 L.A. Sternberger, Immunocytochemistry. 2nd edn. John Wiley, New York 1979.

Stereological analysis of thyroid follicle structure

C. Penel, J.-B. Rognoni, D. Durieu and C. Simon[1]

Laboratoire d'Endocrinologie Cellulaire, Université de Provence, F-13331 Marseille Cedex 3 (France), 19 May 1980

Summary. Besides a possible bias induced by experimental design, some difficulties inherent in stereological analysis appear during thyroid morphometric investigations. These technical considerations are discussed in the light of the follicle size distribution of the 2 lobes of a rat thyroid.

The thyroid gland is composed of a set of convex entities of different diameters; the follicles, which consist of a shell of epithelial cells surrounding a colloid lumen. In order to study the action of these follicles as functional units in the mechanism of iodine turnover and hormone secretion, their size distribution must be determined. Owing to technical difficulties, little work has been carried out to determine thyroid follicle size distribution[2-4]. With the exception of fixation artefacts recently outlined by Denef et al.[5], most of the bias and difficulties appearing during thyroid stereological analysis have not yet been considered or quantified; bias is caused by the non-sphericity of the follicles, underestimation of the number of small diameter follicle sections, statistical fluctuations resulting from the sampling procedures, and the various merits and limits of parametric and nonparametric methods. These technical points will be developed in this note together with the stereological analysis of the 2 lobes of a rat thyroid.

Experimental design. The 2 thyroid lobes of a rat fed on an iodine-rich diet of the industrial type were fixed in Bouin's fluid, dehydrated in alcohol and embedded in paraplast. From each lobe, 9 slices of thickness t = 5 µm, separated by a distance of 300 µm, were systematically taken. The 1777 (left lobe) and 1772 (right lobe) areas of the follicle sections were then measured by planimetry.

Stereological analysis. As a general rule, large follicles are found at the periphery of each lobe of the thyroid whereas all the other sizes are located inside the gland. It is assumed that the centers of these follicles are positioned, inside their respective spaces of distribution, according to the Poisson process[6]. To obtain information about the average follicle structure with minimal sample variance, slices were chosen perpendicular to the greatest axis of each lobe[7,8].

The thyroid follicles are convex entities of tetrakaidecaedral shape. In order to determine their size distribution, a simple

Mean diameter x (µm) and standard deviation Sx (µm) of the follicle size distribution of the 2 lobes of a rat thyroid obtained by the nonparametric and the parametric methods

	Left lobe		Right lobe	
	$\bar{x} \pm \sqrt{\text{var } \bar{x}}$	$Sx \pm \sqrt{\text{var } Sx}$	$\bar{x} \pm \sqrt{\text{var } \bar{x}}$	$Sx \pm \sqrt{\text{var} Sx}$
Nonparametric method	89.0 ± 3.7	35.0 ± 2.2	78.8 ± 3.2	34.4 ± 1.8
Parametric method	87.5 ± 1.7	34.5 ± 1.0	77.5 ± 1.5	32.27 ± 0.9

system has been introduced as suggested by Weibel[9]; the follicles have been described by spheres of equal volume which are called 'volume equivalent spheres'.

The size distribution R3(x) of the spherical entities of diameter x contained in a unit volume is related[10] to the size distribution of sections R2(x) observed on a slice (unit surface) of thickness t by the equation:

$$R2(x)=(\bar{x}+t)^{-1}\left(\int_x^{\infty} x\,(y^2-x^2)^{-1/2}\,R3(y)\,dy+t\,R3(x)\right) \quad (1)$$

where $\bar{x}$ is the mean diameter of the spheres. Before applying equation (1), it is necessary to correct the bias introduced by considering the follicles as spheres. Equation (1) also applies[11] to the connection between a bi-dimensional distribution (circles) and a one-dimensional distribution (random linear intercept lengths of the spherical profils with a network of straight lines used as a linear probe[9]). After measuring the areas of the follicle sections observed on the slices, we have calculated their equivalent diameter (diameter of a circle of the same area). In this manner, the distribution **R2** (matrix notation) with its estimate dispersion matrix **VR2** is obtained[12-14].

Applying equation (1) with **R2** gives the theoretical one-dimensional distribution **R1C**:

$$R1C(x)=(\bar{x})^{-1}\int_x^{\infty} x\,(y^2-x^2)^{-1/2}\,R2(y)\,dy \quad (2)$$

(In this case t = 0). The follicle sections were then sampled by a linear probe. From 5 samples (histograms) of about 600 linear intercepts, the experimental one-dimensional distribution **R1E** (mean histogram) with its dispersion matrix **VR1E** have been estimated following standard statistical procedures (see Danieli[14], p. 55, for example). Without bias, **R1C** and **R1E** would be statistically identical. In fact, **R1C** appears as the homothetic of **R1E** by ratio k^{-1}. In matrix notation, that is expressed by the relation:

$$\mathbf{R1E}(x)=\mathbf{R1C}(k^{-1}x) \quad (3)$$

This empirical relationship characterizes the bias induced by the substitution of follicles by spheres when applying equation (1). Factor k is determined by minimizing the cost function:

$$S1=[\mathbf{R1E}(x)-\mathbf{R1C}(k^{-1}x)]^T\,\mathbf{VR1E}(x)^{-1}[\mathbf{R1E}(x)-\mathbf{R1C}(k^{-1}x)] \quad (4)$$

with the simplex algorithm[15].

To determine the follicle size distribution **R3**, we then applied equation (1) with the corrected distribution **R2E**(x) = **R2**(kx) (equation (5)); a justification of this empirical relationship has been given by Schuckher and Svenska[11]. Resolution of equation (1) gives a linear system[13,16]:

$$\mathbf{R3}=\mathbf{A}^{-1}\mathbf{R2E} \quad (6)$$

and

$$\mathbf{VR3}=\mathbf{A}^{-1}\mathbf{VR2E}(\mathbf{A}^{-1})^T \quad (7)$$

R3 is obtained in histogram form (nonparametric method). **VR3** is the dispersion matrix of **R3**. **VR2E** is the dispersion matrix of **R2E** deduced from **VR2** by the relation **VR2E**(x) = **VR2**(kx). The matrix **A** is available from the authors.

It is difficult to detect on slices, the tangentially sectioned follicles among the thyroid cellular mass. This results in an underestimation of the size of the smallest **R2E** diameter classes leading to negative values (by error transmission) for the corresponding **R3** classes. A threshold measurement h has been introduced. This parameter is characterized so that random interceptions of a sphere of diameter y will give rise to sections of diameter x with $2\sqrt{h(y-h)} \leqq x \leqq y$. See Weibel and Paumgartner[17] for geometrical illustration. Equation (1) becomes:

$$R2(x)=(\bar{x}+t-2h)^{-1}\left(\int_x^{x^2/(4h)-h} x\,(y^2-x^2)^{-1/2}\,R3(y)\,dy+t\,R3(x)\right) \quad (8)$$

Parameter h is determined so that negative values are not obtained for **R3**. The thyroid follicle size distribution was then described by a lognormal law (parametric method):

$$R3C(x,\theta)=(x\,s\sqrt{2\pi})^{-1}\exp-\frac{1}{2}\left(\frac{\log x-m}{s}\right)^2 \quad (9)$$

The identification of the parameters $\theta(m,s)$ is obtained by minimizing the cost function:

$$S2=[\mathbf{R2E}-\mathbf{R2C}]^T\,\mathbf{VR2E}^{-1}[\mathbf{R2E}-\mathbf{R2C}] \quad (10)$$

with the simplex algorithm[15]. $R2C(x,\theta)$ is obtained from $R3C(x,\theta)$ by applying equation (8). The experimental **R2E** distribution constitutes a vector of random variables distributed according to a multinomial law[12]. For a sample sufficiently large in size, and provided the assymptotic

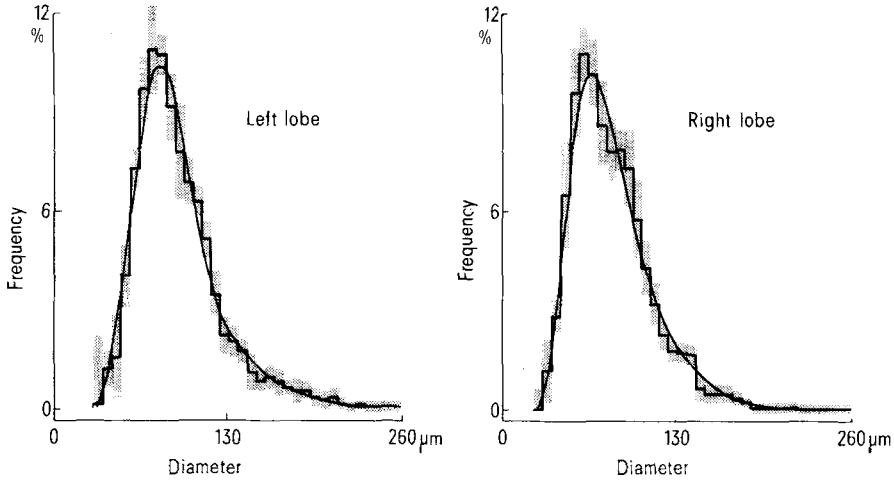

Follicle size distributions of the 2 lobes of a rat thyroid. The histograms have been obtained by the non-parametric method, the size of each class being given with SD (dashed area). The curves depict the log-normal distributions obtained by the parametric method, where parameters are: left lobe $m=4.40\pm0.02$, $s=0.380\pm0.007$; right lobe $m=4.27\pm0.02$, $s=0.400\pm0.006$.

Gauss model for this law is chosen and, if like Nicholson[18] we consider that **R2E** constitutes a vector of independent variables, then minimization of S2 offers maximum likelihood estimation for the parameters[19]. S2 can then be considered as a random variable distributed according to a χ^2 law with n-3 degrees of freedom (histogram with n classes and 2 estimated parameters[20]). This χ^2 statistics has been used as a test of goodness of fit to the data. An estimate of the dispersion matrix of the parameters θ (m, s) is obtained by the inversion of the Hessian matrix[21].

The estimators (and their variances) of the mean $\bar{x}$ (var$\bar{x}$) and of the standard deviation Sx (varSx) of the follicle size distributions have been obtained by the relations:

$$\textit{Nonparametric method: } \bar{x} \simeq \sum_{i=1}^{n} x_i R3(x_i), \quad \mathrm{var}\bar{x} \simeq \sum_{i=1}^{n} x_i^2 VR3(x_i),$$

$$Sx \simeq \left(\sum_{i=1}^{n} (x_i - \bar{x})^2 R3(x_i) \right)^{1/2}$$

$$\mathrm{var}Sx \simeq \frac{1}{4\, Sx^2} \sum_{i=1}^{n} (x_i - \bar{x})^4 \, VR3(x_i)$$

where x_i is the mid-abscissa and VR3 (x_i) the variance of the size of each class i of the histogram.

Parametric method: $\bar{x} \simeq \exp(m + 1/2\, s^2)$, $\mathrm{var}\bar{x} \simeq \exp(2m + s^2)$ (varm $+ s^2$ vars), $Sx \simeq \exp(m + 1/2\, s^2)(\exp(s^2) - 1)^{1/2}$

$\mathrm{var}Sx \simeq \exp(2m + s^2)\ ((\exp(s^2) - 1)\ \mathrm{varm} + s^2 (\exp(s^2) - 1)^{-1} (2 \exp(s^2) - 1)^2$ vars)

where varm and vars are the estimate variances of m and s.

Results and discussion. Recently, Denef et al.[5] have shown that Bouin fixation and paraplast embedding induced the largest shrinkage effect in thyroid lobes preparation, so that flattened follicles result. This method of fixation has been chosen to quantify, in this extreme case, the bias introduced by the non-sphericity of the follicles. These authors have also shown that a single slice, perpendicular to the greatest axis of the lobe and excluding the poles of the gland, gives a distribution of sections which is representative of the whole lobe. To evaluate sampling fluctuations only, without addition of morphological variations between animals, we have sectioned systematically the 2 lobes of a single animal. The chosen interval of section, greater than the diameter of the largest follicle, gives the less noisy sampling for a given number of slices[13,22].

The results of the stereological analysis are presented in the table (parameters) and in the figure (follicle size distributions). The coefficient estimated to correct the bias introduced by the non-sphericity of the follicles is similar for the 2 lobes: left lobe k = 1.086, right lobe k = 1.098. These values are very near the value k = 1.11 used to correct the bias introduced by approximating the tetrakaidecaedron as a sphere. Follicle growth is subjected both to the necessity of filling the available space and to the demand for minimal surface tension. Therefore, if the follicle shape has been partly modeled by a shrinkage effect, it must also reflect an equilibrium shape (tetrakaidecadron) which is relatively widespread in other matrices such as alloy[23] or cellular masses in plants[24].

The threshold measurement: left lobe h = 3.25 µm, right lobe h = 2.10 µm is a secondary parameter introduced to correct the bias induced by the underestimation of the size of the smallest section diameter classes. For estimation purposes, the follicles have been considered to be spherical and have equivalent diameters determined by equation (5). Thus, what is in fact obtained for this parameter is a global mean value for the whole set of sections. In this study, these values represent approximately half the mean cell height of the follicles.

The 2 methods used for thyroid follicle size determination are complementary; each has advantages and disadvantages. The nonparametric method is simple and can be applied whatever the shape of the distribution; it is also easily programmable on minicomputers. Nevertheless, its use necessitates a compromise between the number of classes in the histogram and the number of measurements[13]. Before applying this method for comparative studies of different physiological states, a control of the fluctuations induced by the sampling procedure (figure) seems essential. However, this method requires an approximation inherent to all non-parametric analysis; the entities of a given class i are considered to have the mean diameter x_i. In the parametric method, this approximation is not introduced and, as the parameters are estimated according to the whole set of classes, they are less sensitive to experimental fluctuations. Therefore, the characteristic parameters of the distributions (mean and standard deviation) are determined with more accuracy (table). Nevertheless, like all iterative techniques, this method is costly in computer time and it might be inapplicable for some distribution shapes[4].

The 2 size distributions of the follicles have the same shape but the distribution in the left lobe is shifted toward the largest diameters when compared to the distribution in the right lobe (table and fig.).

This difference is not induced by local morphological heterogeneity; indeed, our sampling method has led us to obtain a representative sample of the follicle size distribution for each lobe. It is not induced by a fixation artefact as the shrinkage effect is the same for the two lobes. As this difference is only valid for the thyroid under investigation, work is in progress to see if such a difference is significant for the rat thyroid and to test its possible influence on thyroid iodine metabolism.

1 Acknowledgments. The authors wish to thank Dr L.M. Cruz-Orive (Department of Anatomy, University of Bern) for suggesting improvements to an early version of the manuscript. This work was supported by a grant of the CNRS (Equipe de Recherche Associée No. 234) and by a grant of the INSERM (Contrat de Recherche Libre No. 79-4-180-3).

2 N. Nadler, C. Leblond and R. Bogoroch, Endocrinology *54*, 154 (1954).
3 C. Simon and B. Droz, J. Physiol., Paris *66*, 51 (1973).
4 A. Cordier, J. Denef and S. Haumont, Cell Tiss. Res. *171*, 449 (1976).
5 J. Denef, A. Cordier, M. Mesquita and S. Haumont, Histochemistry *63*, 163 (1979).
6 W. Nicholson, J. Microsc. *113*, 223 (1978).
7 R. Miles and P. Davy, J. Microsc. *107*, 211 (1976).
8 R. Miles and P. Davy, J. Microsc. *110*, 27 (1977).
9 E. Weibel, Stereological methods, vol. 1. Academic Press, London 1979.
10 P. Goldsmith, Br. J. appl. Phys. *18*, 813 (1967).
11 F. Schuckher and A. Svenska, in: Microscopie quantitative. Ed. R. De Hoff and N. Rhines. Masson, Paris 1972.
12 C. Penel and C. Simon, C. r. Acad. Sci., Paris *279*, 513 (1974).
13 C. Penel and C. Simon, J. Microsc. Biol. cell. *26*, 107 (1976).
14 P. Dagnelie, Analyse statistique à plusieurs variables. Les Presses Agronomiques de Gembloux, 1975.
15 J. Nedler and R. Mead, Comput. J. *7*, 308 (1965).
16 L. Cruz-Orive, J. Microsc. *112*, 153 (1977).
17 E. Weibel and D. Paumgartner, J. Cell. Biol. *77*, 584 (1978).
18 W. Nicholson, J. Microsc. *107*, 323 (1976).
19 H. Britt and L. Luecke, Technometrics *15*, 233 (1979).
20 M. Kendall and A. Stuart, The advanced Theory of Statistics, Vol. 2. C. Griffin, London 1973.
21 M. Bartholomew-Biggs, Math. Programming *12*, 67 (1977).
22 C. Penel and C. Simon, C. r. Acad. Sci., Paris *281*, 2021 (1975).
23 C. Smith, Metal Interface. American Society for Metal, Cleveland, Ohio 1952.
24 T. Allen and C. Potten, Nature *264*, 545 (1976).